Fish and Shellfish Immunology 84 (2019) 587–598

Contents lists available at ScienceDirect

Fish and Shellfish Immunology

journal homepage: www.elsevier.com/locate/fsi

Full length article

The modulation of Smac/DIABLO on mitochondrial apoptosis induced by LPS in *Crassostrea gigas*

Zhao Lv[a,c], Xiaorui Song[b,d], Jiachao Xu[a,c], Zhihao Jia[a,c], Bin Yang[a,c], Yunke Jia[a,c], Limei Qiu[a], Lingling Wang[b,d,e], Linsheng Song[b,d,e,*]

[a] Key Laboratory of Experimental Marine Biology, Institute of Oceanology, Chinese Academy of Sciences, Qingdao, 266071, China
[b] Laboratory of Marine Fisheries Science and Food Production Processes, Qingdao National Laboratory for Marine Science and Technology, Qingdao, 266235, China
[c] University of Chinese Academy of Sciences, Beijing, 100049, China
[d] Liaoning Key Laboratory of Marine Animal Immunology, Dalian Ocean University, Dalian, 116023, China
[e] Liaoning Key Laboratory of Marine Animal Immunology& Disease Control, Dalian Ocean University, Dalian, 116023, China

ARTICLE INFO

Keywords:
Mitochondrial pathway
Smac/DIABLO
LPS
Primary cultured hemocytes
C. gigas

ABSTRACT

The mitochondrial pathway of apoptosis is well studied as the major mechanism of physiological cell death in vertebrates. In the present study, a second mitochondria-derived activator of caspases (Smac)/direct inhibitor of apoptosis-binding protein (IAP) with low pI protein (DIABLO) (designated as *Cg*Smac) was identified from oyster *Crassostrea gigas*. The open reading frame of *Cg*Smac was of 966 bp nucleotides encoding a predicted polypeptide of 321 amino acids with a conserved Smac/DIABLO domain containing a potential IAP-binding motif of VMPV. *Cg*Smac proteins were distributed in hemocytes and co-localized with mitochondria. Western blotting analysis revealed that *Cg*Smac proteins mainly existed in the dimer form in hemocytes, and the monomeric precursors and mature monomers were also detected. After lipopolysaccharide (LPS) stimulation, the mRNA expression of *Cg*Smac in hemocytes was significantly up-regulated and peaked at 6 h (12.26-fold, $p < 0.05$), and the protein level of its dimers was significantly up-regulated at 6 h, 12 h, 24 h, and 48 h, while that of *Cg*Smac monomers was up-regulated at 6 h, 12 h and down-regulated at 24 h, 48 h. The decrease of mitochondrial membrane potential indicated that the occurrence of early stage of apoptosis in primary cultured hemocytes was induced by LPS, and RNA interference (RNAi) of *Cg*Smac could not rescue this decrease. The caspase-3 activity in primary cultured hemocytes was significantly suppressed after RNAi of *Cg*Smac. Correspondingly, the total apoptotic rate of primary cultured hemocytes was also significantly suppressed in ds*Cg*Smac + LPS group (31.57%) compared to dsEGFP + LPS group (40.27%, $p < 0.05$), which in turn demonstrated the conserved pro-apoptotic function of *Cg*Smac. Furthermore, the early apoptotic rate (10.4% vs. 8.5%, $p < 0.05$) was significantly higher in dsCgSmac + LPS group than that of dsEGFP + LPS group, while the necrosis (7.7% vs. 10.0%, $p < 0.05$) and late apoptotic rates (13.4% vs. 21.9%, $p < 0.05$) were lower in ds*Cg*Smac + LPS group than those of dsEGFP + LPS group. Collectively, *Cg*Smac could activate mitochondrial apoptosis pathway by promoting caspase-3 activity in oyster hemocytes against exogenous LPS invasion. These results provided new insights on oyster apoptosis and the immune defense mechanisms in invertebrates.

1. Introduction

Apoptosis, also defined as programmed cell death, is a cellular process to maintain the cell numbers of multicellular organisms, which plays a key role in the developments of tissue and organ, homeostasis maintenance as well as immune defense [1,2]. In general, there are two best-understood activation mechanisms for apoptosis called the extrinsic pathway and the intrinsic pathway (also called the mitochondrial pathway) [3]. The extrinsic pathway is activated by extracellular ligands binding to cell-surface death receptors, which lead to the formation of the death-inducing signaling complex [4]. The mitochondrial pathway is activated by intracellular signals generated when cells are stressed by DNA damage, the arrest of cell cycle, the accumulation of toxins, ATP exhaustion, immune stimulations and etc. [5]. During this process, the mitochondrial membranes become more permeable because of dissipation of mitochondria membrane potential, accompanying with the release of some mitochondrial proteins into cytoplasm [6]. These proteins, including cytochrome C, apoptosis-inducing factor

* Corresponding author. Liaoning Key Laboratory of Marine Animal Immunology, Dalian Ocean University, Dalian, 116023, China.
E-mail address: lshsong@dlou.edu.cn (L. Song).

https://doi.org/10.1016/j.fsi.2018.10.035
Received 2 September 2018; Received in revised form 11 October 2018; Accepted 13 October 2018
Available online 15 October 2018

(AIF), second mitochondria-derived activator of caspases (Smac)/direct inhibitor of apoptosis-binding protein (IAP) with low pI protein (DIABLO), endonuclease G (EndoG) and B-cell lymphoma 2 inhibit of transcription (BitL), can further accelerate the induction of apoptosis [2,5,7].

Smac/DIABLO is an important pro-apoptotic molecule to promote apoptosis by attenuating the inhibitory effect of IAPs on caspases. The process of apoptosis is performed by caspases, which are centrally located in the apoptosis mechanism of both extrinsic pathway and mitochondrial pathway [8,9]. However, caspases are precisely regulated by some molecules during apoptosis [10]. For example, IAPs are a large family proteins which functionally inhibit the activity of apoptotic executors of caspase-3 and caspase-9, and negatively regulate apoptosis [11]. In contrast, this inhibitory effect can be eliminated by other molecules called IAP-binding proteins, such as Smac/DIABLOs, Grim, Hid and etc. [12]. These molecules have a hydrophobic tetrapeptide of AVPI or homologous sequences, which endows them with the binding and blocking activities to IAPs [13]. Smac/DIABLOs are reported as IAPs in the forms of monomer and dimer, and dimer is the mainly active form to exhibit biological functions to promote apoptosis [14]. They are normally located in the mitochondria, and released into the cytoplasm as active dimer form when cells receive apoptotic signals [15]. To a certain extent, Smac/DIABLO released from mitochondria is an important factor to determine cell apoptosis or survival.

In mammals, accumulating evidences reveal that apoptosis-related molecules can respond against immune stresses and initiate the apoptosis of immunocytes, which link the processes of cell apoptosis and immune response. For example, the receptor-interacting protein-1 (RIP1), caspase-8 and RIP3 are found to activate NF-κB and caspase-1, and contribute to the apoptosis of mice macrophages without inflammation during the infection with *Yersinia pestis* [16]. Tumor necrosis factor alpha (TNF-α) are abundantly produced through the autocrine from macrophages and induce apoptosis during exogenous lipopolysaccharide (LPS) invasion [17]. When apoptosis occurs, the further spreading of intracellular pathogens is prevented [18]. In invertebrates, caspase-3 in *C. gigas* is demonstrated with enzymatic activity to mediate apoptosis of hemocytes, as well as with the function of pattern recognition receptor (PRR) to sense intracellular LPS [19]. In *Apostichopus japonicas*, the mRNA expression levels of four caspases are up-regulated during the challenge of *Vibrio splendidus*, suggesting that they are involved in immune response against pathogen infection besides apoptotic cascade signaling pathway [20]. Many other apoptosis-related molecules are also found to sense immune stresses in invertebrates, but the underlying mechanisms of their dual role remained to be further investigated.

The pacific oyster *C. gigas*, a kind of worldwide economic mollusk, inhabits in the intertidal zone, which has to cope with harsh and dynamically changing environments. Multi-omics data reveal that oyster has developed a sophisticated defense system, among which apoptosis is an important way to maintain homeostasis [21]. Analysis of oyster genome indicates that there are numerous apoptosis-related genes, among which caspase-1, caspase-3, caspase-8, and IAP2 have already been identified and proved to be functional in immune process [19,22–24]. In addition, a unique mitochondrial apoptosis pathway has been reported in oyster [25]. Although lack of B cell lymphoma-2 (Bcl-2) homology 3-only subfamily members (BH3) and apoptotic protease activating factor-1 (Apaf-1), the oyster mitochondrial apoptosis pathway could be activated by caspase-3 after the release of mitochondrial pro-apoptotic factor cytochrome C [25]. In the present study, another mitochondrial pro-apoptotic factor, Smac/DIABLO (designated as *Cg*Smac), was identified from pacific oyster *C. gigas*. The main objectives of this study were (1) to characterize the structural and evolutionary features of *Cg*Smac, (2) to investigate its role in LPS-induced apoptosis, and (3) hopefully to provide more evidence about the molecular mechanisms of apoptosis and the association between immune process and apoptosis in oyster.

2. Materials and methods

2.1. Animals

Adult oysters, two-year-old with average length of 11.0 cm, were taken from a local farm in Qingdao, China. Before the experiment, oysters were cultured in tanks filled with aerated seawater for seven days. The water was changed and oysters were fed with powdered spirulina after being washed by a 180 mesh filter every day.

Six-week-old female mice, employed for preparation of polyclonal antibodies, were purchased from the Qingdao Institute of Drug Control in Shandong Province, China, and raised in laboratory environment for one week prior to use. All the animal experiments were conducted according to the regulations of local and central government.

2.2. The analysis of *Cg*Smac sequence and structure

The sequence information of *Cg*Smac (XM_011417608.2) and Smac/DIABLOs from other species was obtained from NCBI (http://www.ncbi.nlm.nih.gov/). The encoding amino acid sequences of *Cg*Smac were generated in the online platform (http://www.bio-soft.net/sms/). In addition, the *Cg*Smac protein domains were predicted by SMART analysis (http://smart.embl-heidelberg.de). The sequence alignment was performed by Clustal ×1.81 algorithm, and the results were generated in ESPript 3.0 (http://espript.ibcp.fr/ESPript/cgi-bin/ESPript.cgi).

2.3. LPS stimulation and sampling from oysters

After temporarily cultured, ninety oysters were divided into two groups. The oysters stimulated with 100 μL of filtered seawater were used as the control group (SW group). The other oysters in the experimental group received the injection with 100 μL of LPS (1 mg/mL, LPS group). Six individuals were randomly sampled from each group at 0, 3, 6, 9, 12, 24 and 48 h post stimulation, and the hemolymph was carefully collected by injection syringe from hematococoel. The hemocytes and serum were separated by centrifugation at 800*g*, 4 °C for 10 min. The samples (gill, mantle, adductor muscle, hepatopancreas, gonad, and hemocytes) were collected from normal oysters to detect the tissue distribution of *Cg*Smac mRNAs.

2.4. RNA extraction, preparation of cDNA library and analysis of real-time quantitative PCR (qRT-PCR)

Total mRNA from samples was extracted by Trizol reagent (Invitrogen). The cDNA was synthesized by using M-MLV reverse transcriptase (Promega) according to the manufacturer's information. The SYBR Green fluorescent *q*RT-PCR technique was used to detect the mRNA expression level of *Cg*Smac. All the reactions were conducted on ABI PRISM 7500 Sequence Detection System (Applied Biosystems). The *C. gigas* elongation factor (*Cg*EF) gene was employed as internal control, and all the used primers were listed in Table 1. The relative mRNA expression level of *Cg*Smac was analyzed by comparative Ct method ($2^{-\triangle\triangle Ct}$ method) [26]. The results were given based on relative mRNA expression level as mean ± S.E.M. (n = 6).

2.5. Preparation of mouse polyclonal antibody

A pair of specific primers of P2 and P3 (Table 1) was designed to obtain Smac/DIABLO domain of *Cg*Smac by using ExTaq DNA polymerase (Takara). After verified by nucleotide sequencing, the correspondingly encoding polypeptides were obtained by the prokaryotic expression system. The recombinant polypeptides were purified and used to prepare mouse polyclonal antibody referred to the previous method [27].

Table 1
Primers used in this study.

Primer purpose	Primer name	Sequence (5′-3′)
Clone primers	P1 (oligo (dT)-adaptor)	GGCCACGCGTCGACTAGTACT$_{17}$
	P2 (*Cg*Smac-F)	ATGCCAGTGGTCAGTGCAATG
	P3(*Cg*Smac-R)	ATCATCCTCCATGGATTCATCCT
RT primers	P4 (*Cg*Smac-RTF)	GCTTCAGAGGCTGCTTAC
	P5 (*Cg*Smac-RTR)	TTCCCATCATCCTTCACTTC
	P6 (*Cg*EF-RTF)	AGTCACCAAGGCTGCACAGAAAG
	P7 (*Cg*EF-RTR)	TCCGACGTATTTCTTTGCGATGT
Recombination primers	P8 (*Cg*Smac-Re-F)	GATATCATGCCAGTGGTCAGTGCAATG
	P9 (*Cg*Smac-Re-R)	CTCGAGATCATCCTCCATGGATTCATCCT
RNA interference	P10 (ds*Cg*Smac-T7-F)	TAATACGACTCACTATAGGGATGCCAGTGGTCAGTGCAATG
	P11 (ds*Cg*Smac-T7-R)	TAATACGACTCACTATAGGGATCATCCTCCATGGATTCATCCT
	P12 (dsEGFP-F)	CGACGTAAACGGCCACAAGT
	P13 (dsEGFP-R)	CTTGTACAGCTCGTCCATGC
	P14 (dsEGFP-T7-F)	TAATACGACTCACTATAGGGATCCGACGTAAACGGCCACAAGT
	P15 (dsEGFP-T7-R)	TAATACGACTCACTATAGGGATCCTTGTACAGCTCGTCCATGC

2.6. Western blotting analysis

The changes of *Cg*Smac on protein level in hemocytes after LPS stimulation were analyzed by western blotting. In brief, the protein extracts of oyster hemocytes were analyzed by SDS-PAGE, and the protein bands were electrophoretically transferred onto nitrocellulose membrane. The membrane was blocked in 5% skim milk powder solution in TBST (50 mM Tris-HCl, 150 mM NaCl, 0.05% Tween-20, pH 7.4) for 2 h, and then incubated with the mouse anti-*Cg*Smac antibody solution (diluted by 1:500, v/v) at 4 °C overnight. After thoroughly washing with TBST for three times, the membrane was incubated with the 1:3000 (v/v) diluted HRP-conjugated IgG (Abcam) for another 2 h. The membranes were finally incubated in western lighting-ECL substrate system (Perkin Elmer) for imaging under ChemiDoc™ MP system (BIO-RAD). The β-tubulin was used as internal reference protein.

2.7. The immunofluorescence assay

The collected hemocytes were washed three times using modified L-15 medium (0.54 g/L KCl, 20.2 g/L NaCl, 0.6 g/L $CaCl_2$, 3.9 g/L $MgCl_2$, 1 g/L $MgSO_4$) [28], and the green fluorescence probes M18 (BestBio) were added into hemocytes suspension to specifically stain mitochondria according to the manufacturer instructions. After extensive washing, 20 μL of resuspension was dropped onto positively charged glass slides for adhesion. The liquid on the slides surface was discarded followed by the fixation in 4% paraformaldehyde for 15 min. After three times washing with PBS (137 mmol/L NaCl, 2.7 mmol/L KCl, 10 mmol/L Na_2HPO_4, 2 mmol/L KH_2PO_4, pH 7.4), 0.5% Triton X-100 was added to hemocytes for permeabilization. Then, 3% BSA in PBS was added to block the nonspecific binding sites for 1 h. Mouse polyclonal IgG against *Cg*Smac was incubated with hemocytes for 1 h, and Alexa Fluor 594 labeled goat anti-mouse IgG was incubated with hemocytes for another 1 h after extensive washing. Hemocytes were further incubated with DAPI for 5 min to stain cell nucleus. Finally, the hemocytes were observed and the fluorescent images were taken using Carl Zeiss LSM 710 confocal microscope (Carl Zeiss).

2.8. Primary oyster hemocytes culture, RNA interference and LPS stimulation

The primary cell culture of oyster hemocytes was conducted according to methods described previously [29]. Briefly, the collected oyster hemocytes were seeded into a 6-well plate (Corning) at the concentration of 5×10^6 cells/well and cultured in modified L-15 medium at 18 °C overnight. Afterwards, *in vitro* knock-down of *Cg*Smac mRNA was conducted by RNA interference according to the previous methods with some modifications [30,31]. In gene interference experiments, 2 μL of double strand RNAs (dsRNAs) including ds*Cg*Smac or dsEGFP (dsEGFP was used in negative control) prepared previously and 5 μL of Lipofectamine 2000 (Invitrogen) were mixed with 100 μL of modified L-15 medium and incubated separately for 5 min. The two mixtures were further mixed together and incubated for another 20 min before adding to l mL of modified L-15 medium. The final mixture was added to each well containing primary hemocytes, and incubated for 24 h for RNA interference. Meanwhile, the primary hemocytes interfered by dsRNAs were treated with LPS (2 μg/mL, Sigma) and sampled post treatment at 0 h and 6 h for subsequent detection of mitochondrial membrane potential, caspase-3 activity, and apoptosis rates. The *q*RT-PCR was used to detect the efficiency of RNA interference. There were three replicates for each sample.

2.9. Detection of mitochondrial membrane potential

The change of mitochondrial membrane potential was detected by JC-1 probes (Beyotime) according to the manufacturer's information. Hemocytes prepared above were incubated with 2 μM JC-1 at 18 °C for 15 min. After centrifugation, the hemocytes pellet were washed and resuspended with fresh modified L-15 medium. Afterwards, 20 μL of suspension were dropped onto glass slides for adhesion, and fixed by 4% paraformaldehyde. Hemocytes were further incubated with DAPI to stain cell nucleus followed by the washing with PBS, and finally the blue, red and green fluorescence of hemocytes were observed and captured using Carl Zeiss LSM 710 confocal microscope (Carl Zeiss).

2.10. Detection of caspase-3 activity in hemocytes

The caspase-3 activity of hemocytes samples were detected using caspase-3 activity assay kit (Beyotime) according to the manufacturer's instructions. In brief, the hemocytes samples prepared in Section 2.8 were harvested by centrifugation, and then the hemocyte pellets were treated with lysis buffer on ice for 15 min, followed by the centrifugation at 12000*g*, 4 °C for 15 min. Immediately, the supernatant was incubated with fluorogenic substrates (Ac-DEVD-pNA) for caspase-3 in dark for 90 min. The absorbance at 405 nm was measured to indicate the fluorescence intensity of free pNA hydrolyzed by caspase-3 from different samples on fluorometer infinite M1000 PRO (TECAN). A unit (U) of caspase-3 activity was defined as the amount of caspase-3 that could cleave 1 nmol of the substrate Ac-DEVD-pNA to produce 1 n mol of pNA in 1 h. There were three replicates for each sample.

2.11. The flow cytometry (FCM) analysis

The apoptosis rates of hemocytes samples prepared in Section 2.8 were also analyzed by flow cytometry. Firstly, the hemocytes were

centrifuged at 800 *g*, 4 °C for 10 min and washed with fresh modified L-15 medium. The hemocytes were then stained using an Annexin V/PI apoptosis kit (Abcam) according to the manufacturer's instructions. All samples were analyzed with a FACS Arial II flow cytometer (Becton Dickinson Biosciences), and there were three replicates for each sample.

2.12. Statistically analysis

Statistical analysis was performed with Origin 8.5.1 software, and results were shown as means ± S.E.M. Multiple group comparisons were executed by one-way ANOVA and Tukey multiple group comparison test using PASW Statistics 18 software. The two-sample Student's *t*-test was used for the comparisons between two groups, and $p < 0.05$ was considered as significant difference.

3. Results

3.1. The features of CgSmac sequence and structure

The open reading frame of *Cg*Smac (XM_011417608.2) was of 966 bp nucleotides encoding 321 amino acids with the molecular weight of 36.04 kDa and theoretical pI of 4.71 (Fig. 1A). A Smac/DIABLO domain was identified at the amino acid of 15–237 (E-value: 1.4e-17) in the deduced amino acid sequence of *Cg*Smac (Fig. 1B). No signal peptide was predicted in *Cg*Smac.

The multiple sequence alignments showed that four conserved amino acid sites of A, V, P and I, marked by blue background in Fig. 2, were conserved as the IAP-binding motif of Smac/DIABLOs in various mammals, such as *Homo sapien* Smac (NP_063940.1), *Rattus norvegicus* Smac (NP_001008293.1), and *Mus musculus* Smac (NP_075721.3) [15]. Whereas, the four corresponding sites in *Gallus gallus* Smac (XP_015131068.1), *Xenopus laevis* Smac (NP_001091439.1), *Danio rerio* Smac (NP_001229963.1), and *Cg*Smac were AVPV, AIPV, AIPF, and VMPV, respectively (Fig. 2), which were different from those in mammals.

3.2. The distribution of CgSmac mRNA transcripts and proteins

The distribution of *Cg*Smac mRNA in different tissues was investigated by *q*RT-PCR. The lowest expression level of *Cg*Smac was

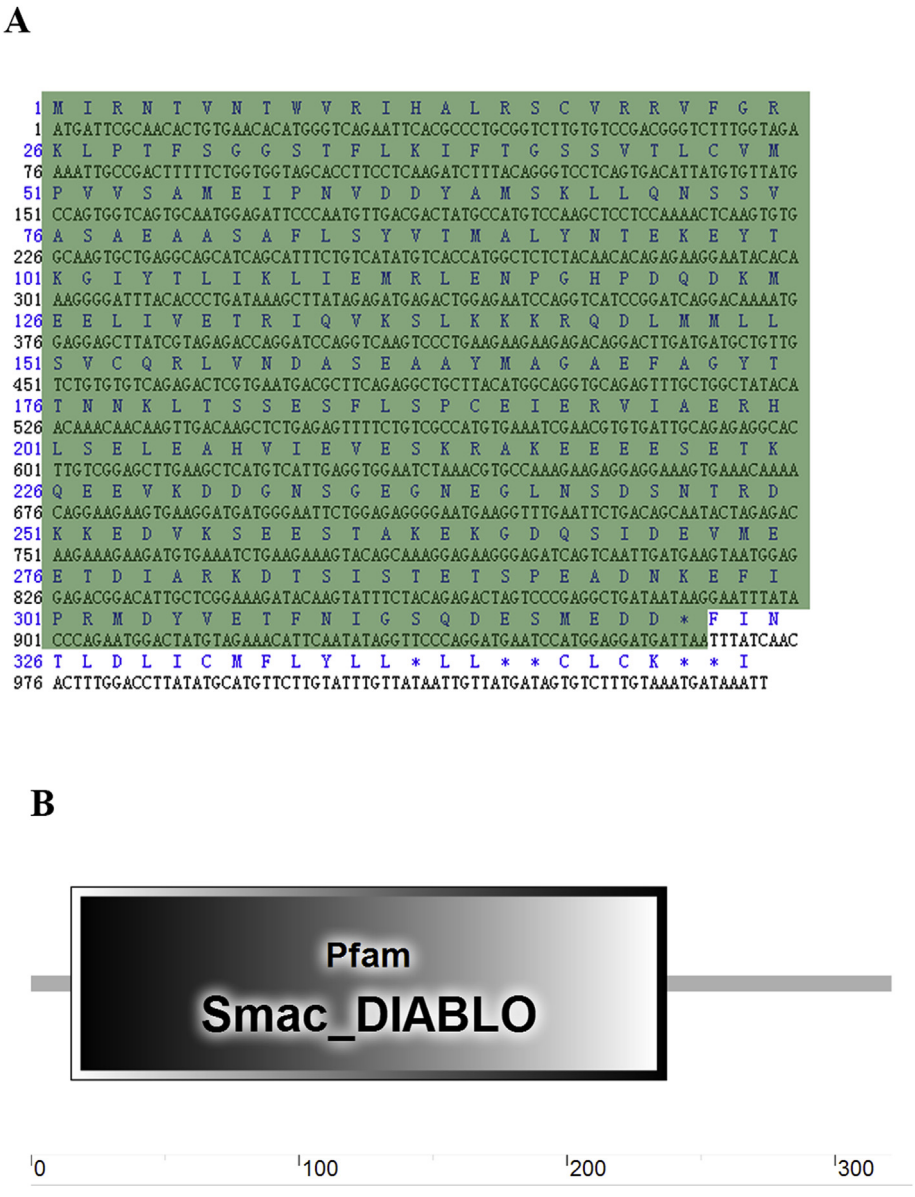

Fig. 1. Sequence features of *Cg*Smac. (A) The sequence of ORF and encoded amino acids. (B) Prediction of protein domains by SMART analysis.

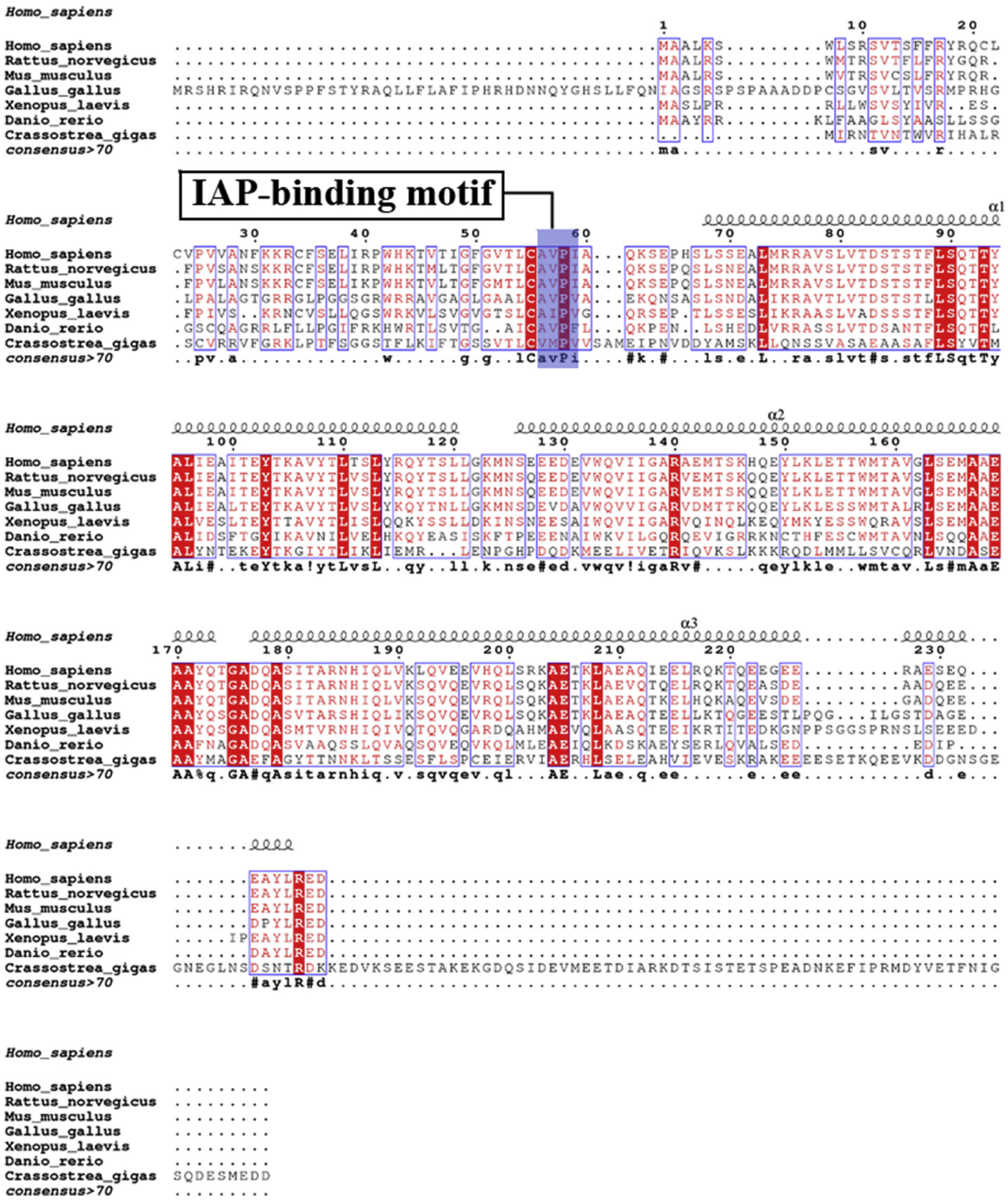

Fig. 2. Multiple sequence alignments of *Cg*Smac with known Smac/DIABLOs from other species: *Homo sapien* Smac (NP_063940.1), *Rattus norvegicus* Smac (NP_001008293.1), *Mus musculus* Smac (NP_075721.3), *Gallus gallus* Smac (XP_015131068.1), *Xenopus laevis* Smac (NP_001091439.1), *Danio rerio* Smac (NP_001229963.1), and *Cg*Smac. Similar (consensus > 70%) amino acids are with red lettering. Gaps are indicated by dashes to improve the alignment. IAP-binding motif of Smac/DIABLOs was marked by blue background. (For interpretation of the references to color in this figure legend, the reader is referred to the Web version of this article.)

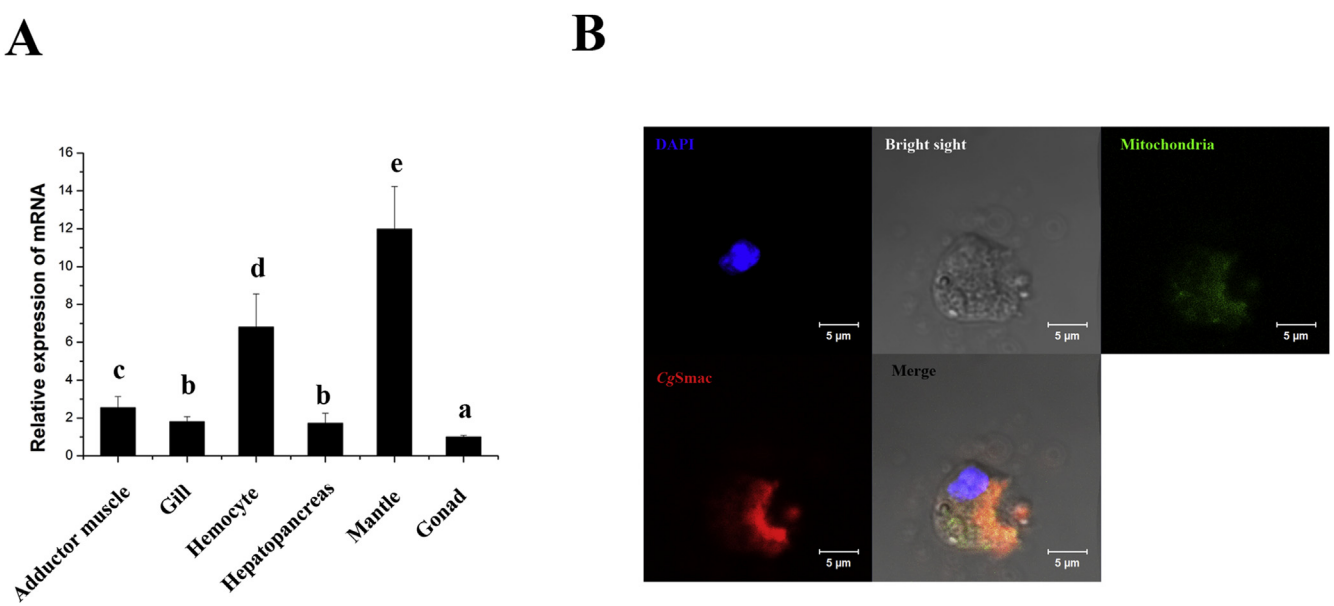

Fig. 3. The distributions of *Cg*Smac mRNA transcripts and proteins. (A) Relative mRNA expression levels of *Cg*Smac in different tissues. Results are shown as means ± S.E.M. (n = 6), and the letters (a, b, c etc.) presented significant differences $p < 0.05$. (B) Localization of *Cg*Smac protein in oyster hemocytes. *Cg*Smac was visualized by Alexa 594-labeled secondary antibody (red color), and the nucleus and mitochondria of hemocytes were stained by DAPI (blue color) and M18 fluorescent dye (green color). Bar = 5 μm. (For interpretation of the references to color in this figure legend, the reader is referred to the Web version of this article.)

observed in gonad, while the highest expression level of *Cg*Smac was observed in mantle which was 11.98-fold of gonad ($p < 0.05$). It was also higher in hemocytes with 6.81-fold of gonad ($p < 0.05$), while relatively lower in hepatopancreas, adductor muscle and gill, which were 1.72-fold ($p < 0.05$), 2.54-fold ($p < 0.05$) and 1.81-fold ($p < 0.05$) of gonad, respectively (Fig. 3A).

The mouse polyclonal antibody against *Cg*Smac was employed in immunofluorescence to investigate the subcellular localization of *Cg*Smac proteins in oyster hemocytes by confocal microscopy (Fig. 3B). The mitochondria was specifically stained by M18 fluorescent dye in green color, and DAPI was used to stain cellular nuclei was stained with DAPI in blue color. The secondary antibody labeled by Alexa Fluor 594 specifically bound to *Cg*Smac protein, and the signal was in red color. The red positive signals of *Cg*Smac proteins were detected in hemocytes, and especially, a great portion of *Cg*Smac proteins were co-localized with the green fluorescently-labeled mitochondria (Fig. 3B).

3.3. The expression pattern of CgSmac mRNA transcripts and proteins after LPS stimulation

The temporal changes of *Cg*Smac in oyster hemocytes at mRNA and protein expression levels after LPS stimulation were examined by *q*RT-PCR and western blotting, respectively. The mRNA expression level of *Cg*Smac was up-regulated at 3 h (2.01-fold, $p < 0.05$), peaked at 6 h (12.26-fold, $p < 0.05$), and then dropped down at 9 h (7.38-fold, $p < 0.05$), 12 h (3.61-fold, $p < 0.05$) and 24 h (1.23-fold, $p < 0.05$) post LPS stimulation, respectively (Fig. 4A). Afterwards, the *Cg*Smac mRNA expression level returned to the normal level at 48 h (1.01-fold, $p > 0.05$) (Fig. 4A).

The western blotting analysis was further performed to investigate the temporal changes of *Cg*Smac at protein level, and three bands were detected from oyster hemocytes (Fig. 4B). The band with the molecular weight about 72 kDa was the dimer of *Cg*Smac protein, and two other protein bands with the molecular weight about 40 kDa were the monomer 1 (M1) and monomer 2 (M2), which were approximately consistent with their predicted molecular weight of 36.04 kDa (Fig. 4B). The band intensity of *Cg*Smac dimer in normal oyster hemocytes (0 h) was calculated as the standard, which was 2.04-fold of M1 ($p < 0.05$), and 2.13-fold of M2 ($p < 0.05$), respectively (Fig. 4C). In addition, the expression level of *Cg*Smac dimers obviously responded to LPS stimulation, and their protein expression levels were significantly up-regulated with the band intensity of 2.13-fold ($p < 0.05$), 1.92-fold ($p < 0.05$), 2.34-fold ($p < 0.05$), and 2.17-fold ($p < 0.05$), at 6, 12, 24, and 48 h post LPS stimulation, respectively, compared to that at 0 h (Fig. 4C). The monomers were also significantly up-regulated at 6 h (M1 with 0.66-fold, $p < 0.05$; M2 with 0.68-fold, $p < 0.05$) and at 12 h (M1 with 0.69-fold, $p < 0.05$; M2 with 0.71-fold, $p < 0.05$), compared to those at 0 h (M1 with 0.49-fold; M2 with 0.47-fold). However, they were relatively down-regulated post LPS stimulation at 24 h (M1 with 0.37-fold, $p < 0.05$; M2 with 0.38-fold, $p < 0.05$) and 48 h (M1 with 0.34-fold, $p < 0.05$; M2 with 0.32-fold, $p < 0.05$), compared to those at 0 h (Fig. 4C).

The changes of intracellular *Cg*Smac proteins after LPS stimulation were visually analyzed by immunofluorescence (Fig. 4D). Because the mRNA expression level of *Cg*Smac peaked at 6 h post LPS stimulation, the hemocyte samples at this point-time were assessed with the untreated and seawater stimulated oysters as blank and negative control (SW group), respectively. The *Cg*Smac proteins were indicated by Alexa Fluor 594 antibody in red color, and the cellular nuclei and mitochondria were stained by DAPI in blue color and M18 fluorescent dye in green color, respectively. No significant changes of mitochondria distribution signals (green color) were observed in the hemocytes among LPS group, blank group and SW group (Fig. 4D). The red fluorescence intensity of *Cg*Smac proteins became obviously stronger in LPS group compared to blank group and SW group, and the red signals of *Cg*Smac proteins were mostly co-localized with mitochondria (green color) (Fig. 4D).

3.4. The effect of LPS stimulation on mitochondrial membrane potential after RNAi of CgSmac

The primary cultured hemocytes interfered by dsRNAs were stimulated again by LPS, and the *Cg*Smac mRNA expression and mitochondrial membrane potential were examined. The ds*Cg*Smac or dsEGFP (negative control) was transfected into the cultured primary hemocytes, and the mRNA expression levels of *Cg*Smac were evaluated by *q*RT-PCR (Fig. 6A). Compared with the dsEGFP group, the mRNA expression level of *Cg*Smac was significantly down-regulated in

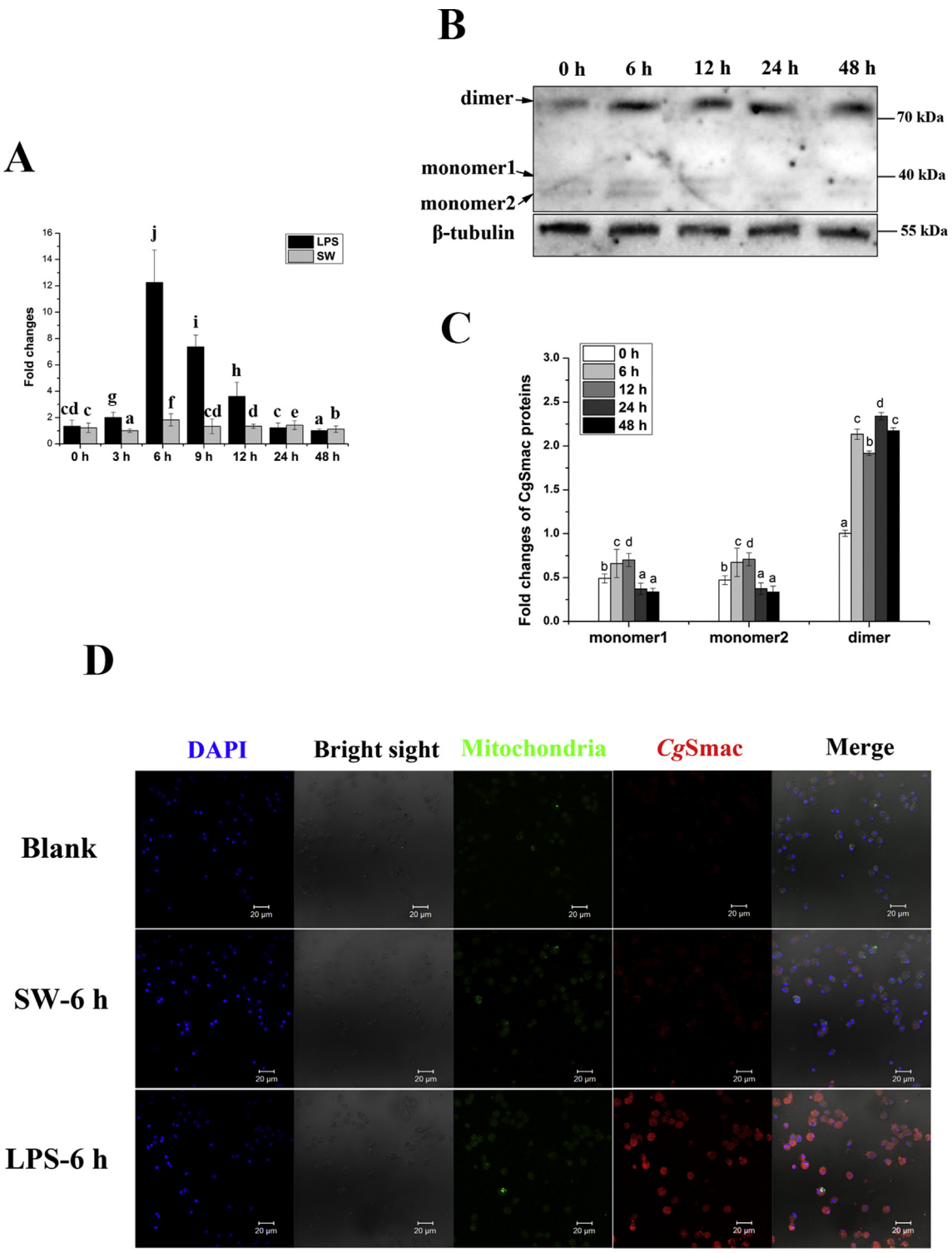

Fig. 4. Changes of *Cg*Smac in hemocytes after LPS stimulation. (A) The temporal changes of *Cg*Smac mRNA expression level in hemocytes post LPS and seawater stimulations. (B) Western blotting analysis of the changes of *Cg*Smac proteins after LPS stimulation. The β-tubulin was used as internal reference protein. (C) Protein band intensity analysis about the changes of *Cg*Smac proteins according to the results of Fig. 4B. The protein expression level of *Cg*Smac is indicated as the intensity ratio of *Cg*Smac to β-tubulin, and then standardized by comparing with the band intensity of *Cg*Smac expression at 0 h. Results are shown as means ± S.E.M. (n = 3), and the letters (a, b, c etc.) presented significant differences $p < 0.05$. (D) Changes of *Cg*Smac proteins after LPS stimulation analyzed by immunofluorescence. Binding of antibody to *Cg*Smac was visualized by Alexa 594-labeled secondary antibody (red color), and the nucleus and mitochondria of hemocytes were stained by DAPI (blue color) and M18 fluorescent dye (green color). Bar = 20 μm. (For interpretation of the references to color in this figure legend, the reader is referred to the Web version of this article.)

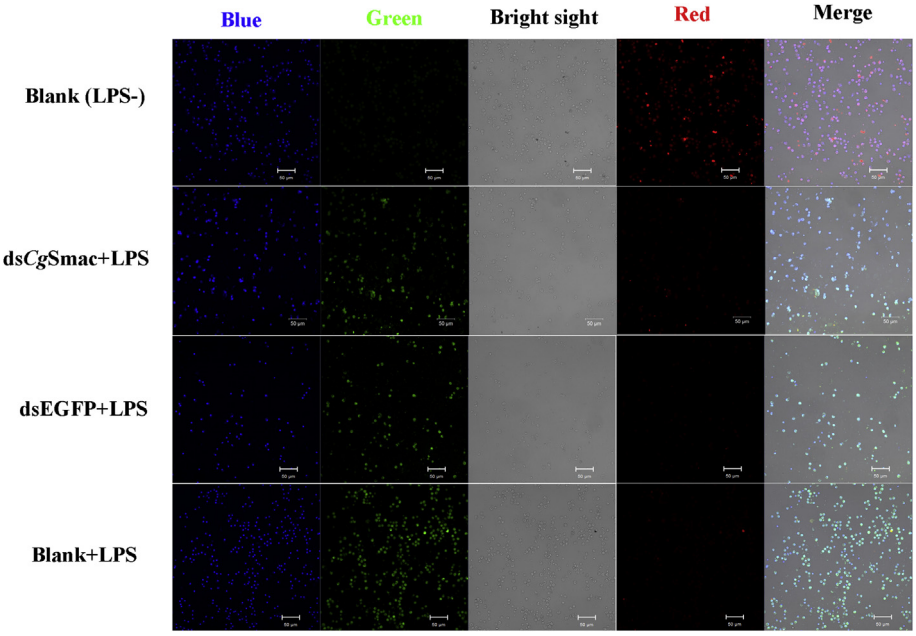

Fig. 5. Assessment of mitochondrial membrane potential by JC-1 staining. Hemocytes interfered by RNAi of *Cg*Smac or untreated were stimulated again by LPS, and JC-1 fluorescence was monitored by confocal microscopy. Bar = 50 μm.

ds*Cg*Smac group, which was 0.26-fold of dsEGFP group ($p < 0.05$) (Fig. 6A). No significant difference was detected between dsEGFP group and blank group (without dsRNAs treatment, dsRNAs$^-$) (Fig. 6A).

The dissipation of mitochondrial membrane potential portending early stages of apoptosis was determined by JC-1 probes after the hemocytes treated with dsRNAs were stimulated by LPS. The fluorescence shift from red to green (or the decrease of the ratio of red to green fluorescence) could be indicated by JC-1 probes when mitochondrial membrane potential occurred dissipation, and the fluorescence intensities of green and red were observed by confocal microscopy (Fig. 5). After LPS stimulation, fewer red fluorescence was detected and the ratio of red to green fluorescence decreased in Blank + LPS group (dsRNAs$^-$ LPS$^+$), ds*Cg*Smac + LPS group (ds*Cg*Smac$^+$ LPS$^+$) and dsEGFP + LPS group (dsEGFP$^+$ LPS$^+$) compared to Blank (LPS-) group (dsRNAs$^-$ LPS$^-$), and the decreased ratio of red to green fluorescence in ds*Cg*Smac + LPS group was not rescued compared to dsEGFP + LPS group (Fig. 5).

3.5. The effect of LPS stimulation on caspase-3 activity after dsRNAi of *CgSmac*

To clarify the function of *Cg*Smac in oyster hemocytes, the caspase-3 activity in the primary cultured hemocytes was determined after the hemocytes interfered by dsRNAs were stimulated again by LPS (Fig. 6B). It showed that there was no significant difference of caspase-3 activity between Blank (LPS-) group (29.93 U/mg protein) and dsEGFP (LPS-) group (dsEGFP$^+$ LPS$^-$, 28.11 U/mg protein, $p > 0.05$). While RNAi of *Cg*Smac could significantly decrease the caspase-3 activity to

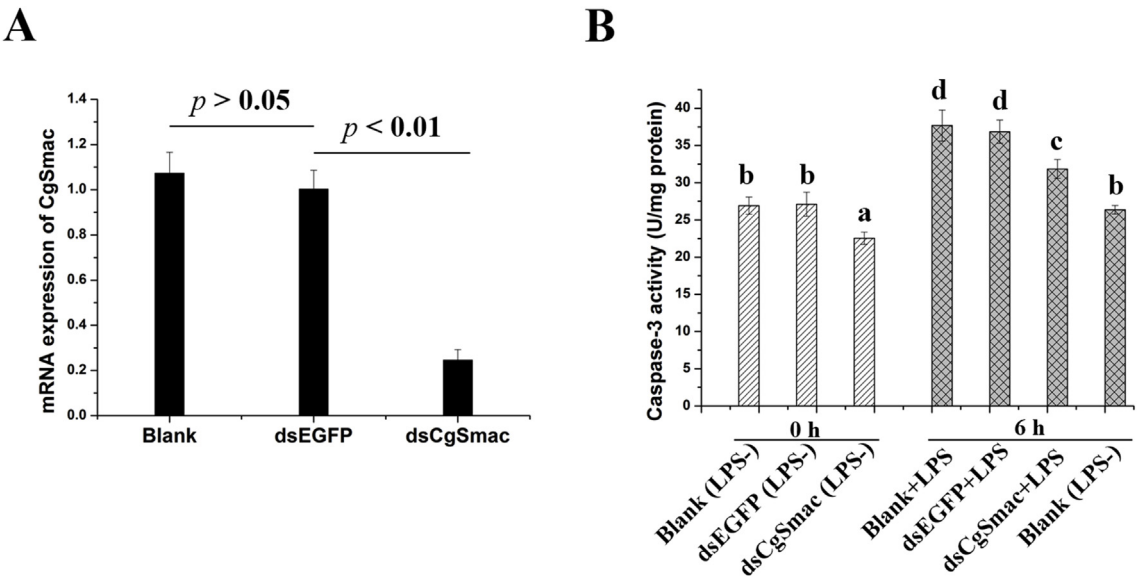

Fig. 6. Changes of caspase-3 activity in primary cultured oyster hemocytes. (A) The changes of *Cg*Smac mRNA transcripts in hemocytes after RNAi. (B) The changes of caspase-3 activity after the hemocytes interfered by dsRNAs or untreated were stimulated again by LPS. Results are shown as means ± S.E.M. (n = 3), and the letters (a, b, c etc.) presented significant differences $p < 0.05$.

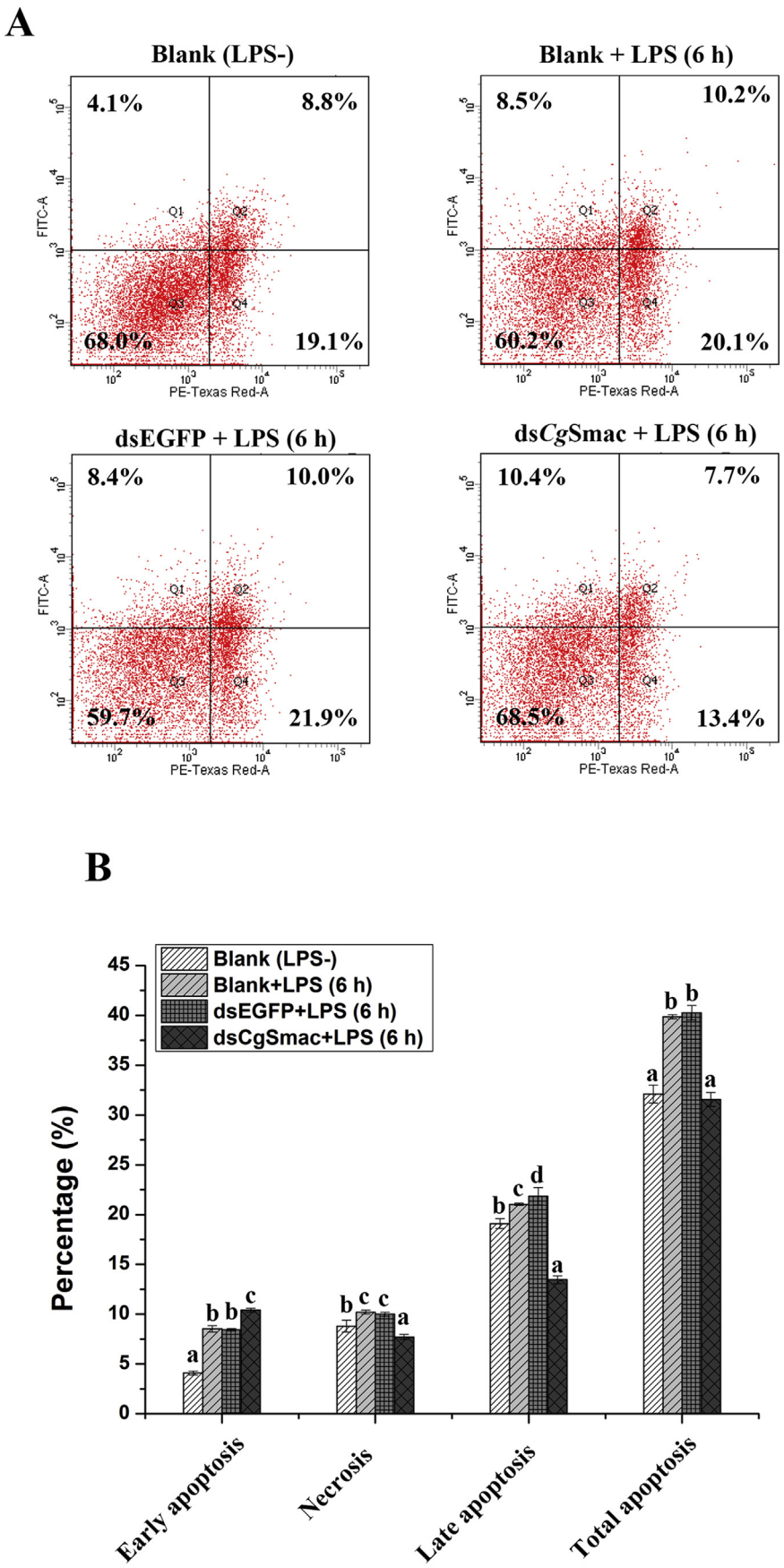

Fig. 7. Apoptosis of primary cultured oyster hemocytes induced by LPS. (A) The apoptotic levels after the hemocytes interfered by dsRNAs were stimulated again by LPS detected by flow cytometry. (B) The percentages of early apoptosis, necrosis, late apoptosis, and total apoptosis gated on Annexin V^+/PI^-, Annexin V^+/PI^+ and Annexin V^-/PI^+. Results are means ± S. E. M. (n = 3), and the letters (a, b, c etc.) presented significant differences $p < 0.05$.

22.55 U/mg protein in ds*Cg*Smac (LPS-) group (ds*Cg*Smac^{+} LPS^{-}) compared to dsEGFP (LPS-) group (28.11 U/mg protein, $p < 0.05$) (Fig. 6B).

The caspase-3 activity was significantly increased to 37.69 U/mg protein in Blank + LPS group compared to Blank (LPS-) group (26.37 U/mg protein, $p < 0.05$) after LPS stimulation of 6 h. No significant difference of caspase-3 activity was observed between dsEGFP + LPS group (36.86 U/mg protein) and Blank + LPS group (37.69 U/mg protein, $p > 0.05$). However, the RNAi of *Cg*Smac significantly decreased the caspase-3 activity to 31.85 U/mg protein in dsEGFP + LPS group compared to dsEGFP + LPS group (36.86 U/mg protein, $p < 0.05$) (Fig. 6B).

3.6. The effect of LPS stimulation on apoptotic level after dsRNAi of *CgSmac*

The apoptotic levels were also detected using flow cytometry after the hemocytes interfered by dsRNAs were stimulated again by LPS (Fig. 7). Annexin V could specifically bind to phosphatidylserine (PS) which appeared on the mitochondrion membrane during early apoptosis, and propidium iodide (PI) was used to stain cellular nuclei of dead apoptotic cells. The total apoptosis rates were equal to the percentage sum of the early apoptosis, necrosis, and late apoptosis. It significantly increased to 39.87% in Blank + LPS group after LPS stimulation of 6 h compared to Blank (LPS-) group (32.10%, $p < 0.05$) (Fig. 7). The total apoptosis rates was 31.57% in ds*Cg*Smac + LPS group, which was significantly lower than that in dsEGFP + LPS group (40.27%, $p < 0.05$) (Fig. 7).

The percentages of hemocytes with PI positive and Annexin V negative signals (necrosis) and hemocytes with Annexin V and PI double positive signals (late apoptosis) in ds*Cg*Smac group were 7.7% and 13.4%, respectively, which were significantly lower than those in dsEGFP + LPS group with the necrosis rate of 10.0% ($p < 0.05$), and the late apoptosis rate of 21.9% ($p < 0.05$), respectively (Fig. 7). They were also significantly lower than those in Blank + LPS group with the necrosis rate of 10.2% ($p < 0.05$), and the late apoptosis rate of 20.1% ($p < 0.05$), respectively (Fig. 7). However, the percentage of Annexin V positive and PI negative hemocytes (early apoptosis) was the highest with 10.4% in the ds*Cg*Smac + LPS group compared to dsEGFP + LPS group (8.4%, $p < 0.05$) and Blank + LPS group (8.5%, $p < 0.05$) (Fig. 7).

4. Discussion

The intrinsic or mitochondrial apoptosis pathway is described by the involvement of mitochondria in apoptotic signaling, and it has been extensively studied in most vertebrates [6,32,33]. During this pathway, many pro-apoptotic signals are converged in mitochondria, inducing the changes of mitochondrial membrane permeability and the release of mitochondria intermembrane proteins, which activate downstream caspase activity to initiate cell apoptosis [5,7]. Although several homologs of mammalian apoptosis-related effectors have been identified in invertebrates, the mechanisms of mitochondrial apoptosis remain to be elaborated [6]. Recently, a unique mitochondrial apoptosis pathway is reported in mollusk *C. gigas* [25]. Although BH3 and Apaf-1 were not annotated in the genome of this animal, the mitochondrial cytochrome C could be released to the cytoplasm after UV-radiation, and subsequently promoted the activities of caspase-3 and caspase-9, eventually triggering cell apoptosis [25]. Smac/DIABLO is a newly discovered mitochondrial intermembrane protein, which parallels to the mitochondrial pro-apoptotic protein cytochrome C to promote apoptosis through different ways [15]. In the present study, a Smac/DIABLO *Cg*Smac was identified from oyster hemocytes, and its roles in mitochondrial apoptosis and immune response were further explored.

Smac/DIABLOs eliminate the inhibitory effects on caspases by interacting with IAPs. In mammals, accumulating evidences reveal that Smac/DIABLOs can interact with a variety of IAPs, including X-linked inhibitor of apoptosis protein (XIAP), cIAP1, cIAP2, melanoma apoptosis protein inhibitor (ML-IAP), and Survivin [12]. Specifically, it has been reported that AVPI, the N-terminal tetrapeptide of Smac/DIABLOs, functions as a conserved IAP-binding motif to bind the surface groove of XIAP-BIR3, forming repulsive force to caspase-9, and attenuates the inhibitory effect of XIAP on caspases [13]. The Smac/DIABLO homologs are not well studied in invertebrates, and only some pro-apoptotic factors, such as Hid, Grim, Reaper and Sickle with IAP-binding motif (AVPI) homologous to mammalian Smac/DIABLOs have been reported to bind IAPs [34]. The tetrapeptide of AVPI or its homologue sequences in IAP-binding proteins is a prerequisite IAP-binding motif among animals [15]. In this study, *Cg*Smac with a conserved Smac/DIABLO domain was demonstrated to promote mitochondrial apoptosis, firstly indicating the existence of Smac/DIABLO in mollusks. Multiple sequence alignments showed that the tetrapeptide of predicted IAP-binding motif in *Cg*Smac was VMPV, which was clearly different from mammalian Smac/DIABLOs and other vertebrates Smac/DIABLOs. Considering that these amino acids were all hydrophobic, aiding Smac/DIABLOs in binding IAPs' hydrophobic groups [13,15], it was speculated that a different and complex binding mechanism existed between *Cg*Smac and large number of IAPs in oyster (IAP families in oyster are highly expanded with a total of 48 genes [21]).

Some apoptosis-related molecules also participate in the immune defense process, which link apoptosis and immunity. LPS is the major component of the outer membrane of Gram-negative bacteria, which can induce the overactive immune system as well as apoptosis [35]. In mammals, TNF-α-dependent apoptosis is reported to withstand against exogenous LPS invasion through PKC/JNK pathway in macrophages [17,36]. In invertebrates, LPS-induced TNF-α factor (LITAF) from snail *Cipangopaludina chinensis* is identified functional in apoptosis, suggesting that TNF-α also plays an important role in defense mechanism against exogenous LPS invasion in this animal [37]. Additionally, poly-U-binding factor 60 kDa (PUF60) from sea cucumber *Stichopus monotuberculatus* intensely respond at transcriptional level against LPS stimulation, and overexpressed PUF60s can induce apoptosis [38]. The caspase-3 in *C. gigas* exhibits the activity to recognize intracellular LPS as well as initiating apoptosis, and oyster hemocytic apoptosis can be hindered by intracellular LPS due to the inhibition of caspase-3 [19], suggesting the complexity between host defense of cell apoptosis and foreign invasion in invertebrates. In the present study, extracellular LPS treatment could induce mitochondrial apoptosis of oyster hemocytes, which was different from the inhibitory effects caused by intracellular LPS in previous study [19]. More importantly, the massive accumulations of *Cg*Smac mRNA transcripts and proteins in hemocytes post LPS stimulation provided the hints for the link between the LPS-induced apoptosis and invertebrate Smac/DIABLO.

In mammals, Smac/DIABLOs promote apoptosis mainly as dimers. Structurally, mammalian Smac/DIABLOs exist in the forms of monomers and dimers [14]. The monomeric precursor of Smac/DIABLO contains a mitochondrial target sequence, which will be excised and become mature Smac/DIABLO (also known as the wild-type Smac/DIABLO) after translocated into mitochondria [14]. With the ability to recognize XIAP-BIR3, the monomers slightly promote pro-caspase activation, while Smac/DIABLO dimer is the major form of Smac/DIABLO, which plays a dual roles in effectively binding XIAP-BIRs to promote the activation of pro-caspase and directly promoting caspase activity [15]. In invertebrates, only some insect IAP-binding proteins such as Hid, Grim, and Reaper are reported to be active as monomers to bind to Diap1 [39]. In the present study, *Cg*Smac proteins were found to exist in three forms with the molecular weight of 36 kDa (two bands) and 72 kDa (one band), which corresponded to the monomeric precursor, mature monomer, and dimer in mammals [14]. The intensity of western blotting band of *Cg*Smac dimer was found to be much higher than that of other two forms, suggesting that *Cg*Smac existed mainly as dimer in oyster hemocytes. The level of *Cg*Smac dimers was persistently

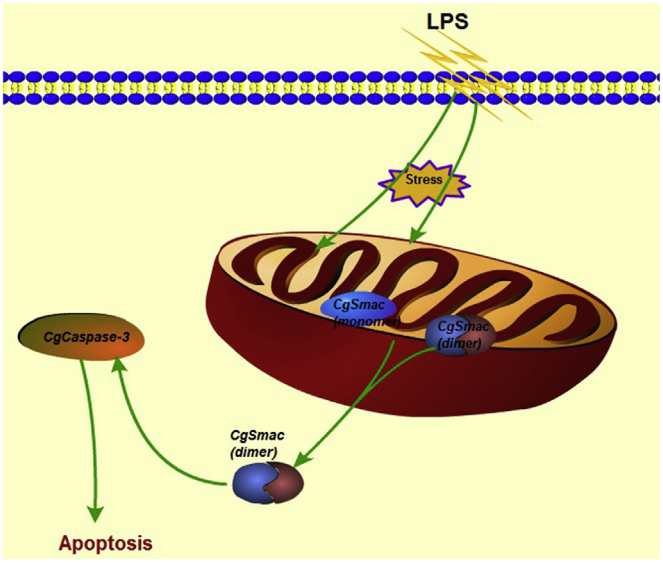

Fig. 8. The conceptual framework of mitochondrial apoptosis pathway centered on *Cg*Smac-caspase-3 axis against stress of exogenous LPS in oyster.

up-regulated after LPS stimulation, and *Cg*Smac monomers were down-regulated during the late stage of LPS stimulation, which might be resulted from a transition from the form of monomer to the mainly functional form dimer of *Cg*Smac.

Smac/DIABLO promotes mitochondrial apoptosis by elevating intracellular caspase-3 activity, which is the central effector of mitochondrial pathway [12,40]. Besides, the increased permeability of the mitochondrial membrane is a prerequisite for Smac/DIABLO to function [5]. In the present study, LPS stimulation on hemocytes significantly decreased the mitochondrial membrane potential, which was similar with previous reports that the increase of mitochondrial membrane permeability occurred at early stage of LPS-induced apoptosis [41]. It indicated that *Cg*Smac release was the downstream effect of increased mitochondrial membrane permeability caused by LPS stimulation, and RNAi of *Cg*Smac did not rescue the decrease of mitochondrial membrane potential. Expectedly, caspase-3 activity of hemocytes was significantly decreased after RNAi of *Cg*Smac regardless of LPS treatment or not, which should the downstream effects of *Cg*Smac release. With the down-regulation of caspase-3 activity, the total cell apoptotic rates were correspondingly decreased. Furthermore, the early apoptotic rate was significantly higher, and the necrosis and late apoptotic rates were lower in ds*Cg*Smac group than those in control group, indicating that RNAi of *Cg*Smac possibly retained the dying hemocytes at early apoptotic stage and partly rescued LPS-induced apoptosis. Collectively, *Cg*Smac release was proved as the downstream effects of increased mitochondrial permeability induced by LPS, in turn promoting caspase-3 activity to induce apoptosis, which provided a new insight on defense mechanism for oyster hemocytes against exogenous LPS invasion.

In summary, *Cg*Smac was identified from oyster with a conserved Smac/DIABLO domain and an IAP-binding motif of VMPV. *Cg*Smac mRNA transcripts were widely detected in various oyster tissues, and *Cg*Smac proteins could co-localize with mitochondria in hemocytes. *Cg*Smac proteins existed in three forms, namely monomer precursor, mature monomer and dimer, and the dimer was the major form of *Cg*Smac *in vivo* to exert the biological function. *Cg*Smac dimers in oyster hemocytes were significantly up-regulated both at mRNA and protein levels after LPS stimulation. The caspase-3 activity of hemocytes significantly reduced after RNAi of *Cg*Smac compared to the control group regardless of LPS treatment or not. In addition, decreased caspase-3 activity caused reduction of cell apoptosis rates, demonstrating the conserved pro-apoptotic function of *Cg*Smac. This study suggested that there might be a mitochondrial apoptosis pathway centered on *Cg*Smac-caspase-3 axis against stress of exogenous LPS in oyster (Fig. 8). These results collectively expanded the knowledge of studies on invertebrate apoptosis, shedding lights on the immune defense mechanism of oyster via apoptosis.

Acknowledgements

The authors are grateful to all the laboratory members for continuous technical advice and helpful discussions. This research was supported by the National Natural Science Foundation of China (No. 31530069), the Research Foundation for Talented Scholars in Dalian Ocean University, AoShan Talents Cultivation Program Supported by Qingdao National Laboratory for Marine Science and Technology (No. 2017ASTCP-OS13), Research Foundation for Distinguished Professor in Liaoning, and earmarked fund (CARS-49) from Modern Agro-industry Technology Research System.

References

[1] C.M. Zmasek, A. Godzik, Evolution of the animal apoptosis network, Cold Spring Harb Perspect. Biol. 5 (2013) a008649.
[2] D.R. Green, P. Fitzgerald, Just so stories about the evolution of apoptosis, Curr. Biol. 26 (2016) R620–R627.
[3] I. Bohm, H. Schild, Apoptosis: the complex scenario for a silent cell death, Mol. Imag. Biol. 5 (2003) 2–14.
[4] S. Elmore, Apoptosis: a review of programmed cell death, Toxicol. Pathol. 35 (2007) 495–516.
[5] J. Estaquier, F. Vallette, J.L. Vayssiere, B. Mignotte, The mitochondrial pathways of apoptosis, Adv. Exp. Med. Biol. 942 (2012) 157–183.
[6] C.E. Bender, P. Fitzgerald, S.W. Tait, F. Llambi, G.P. McStay, D.O. Tupper, et al., Mitochondrial pathway of apoptosis is ancestral in metazoans, Proc. Natl. Acad. Sci. U. S. A. 109 (2012) 4904–4909.
[7] P. Ludovico, F. Rodrigues, A. Almeida, M.T. Silva, A. Barrientos, M. Corte-Real, Cytochrome c release and mitochondria involvement in programmed cell death induced by acetic acid in *Saccharomyces cerevisiae*, Mol. Biol. Cell 13 (2002) 2598–2606.
[8] T.J. Fan, L.H. Han, R.S. Cong, J. Liang, Caspase family proteases and apoptosis, Acta Biochim. Biophys. Sin. 37 (2005) 719–727.
[9] S. Shalini, L. Dorstyn, S. Dawar, S. Kumar, Old, new and emerging functions of caspases, Cell Death Differ. 22 (2015) 526–539.
[10] Y. Shi, Mechanisms of caspase activation and inhibition during apoptosis, Mol. Cell 9 (2002) 459–470.
[11] A.M. Verhagen, E.J. Coulson, D.L. Vaux, Inhibitor of apoptosis proteins and their relatives: IAPs and other BIRPs, Genome Biol. 2 (2001) Reviews 3009.
[12] E.N. Shiozaki, Y. Shi, Caspases, IAPs and Smac/DIABLO: mechanisms from structural biology, Trends Biochem. Sci. 29 (2004) 486–494.
[13] G. Wu, J. Chai, T.L. Suber, J.W. Wu, C. Du, X. Wang, et al., Structural basis of IAP recognition by Smac/DIABLO, Nature 408 (2000) 1008–1012.
[14] C. Du, M. Fang, Y. Li, L. Li, X. Wang, Smac, a mitochondrial protein that promotes cytochrome c-dependent caspase activation by eliminating IAP inhibition, Cell 102 (2000) 33–42.
[15] J. Chai, C. Du, J.W. Wu, S. Kyin, X. Wang, Y. Shi, Structural and biochemical basis of apoptotic activation by Smac/DIABLO, Nature 406 (2000) 855–862.
[16] D. Weng, R. Marty-Roix, S. Ganesan, M.K. Proulx, G.I. Vladimer, W.J. Kaiser, et al., Caspase-8 and RIP kinases regulate bacteria-induced innate immune responses and cell death, Proc. Natl. Acad. Sci. U. S. A. 111 (2014) 7391–7396.
[17] J. Xaus, M. Comalada, A.F. Valledor, J. Lloberas, F. Lopez-Soriano, J.M. Argiles, et al., LPS induces apoptosis in macrophages mostly through the autocrine production of TNF-alpha, Blood 95 (2000) 3823–3831.
[18] C.V. Nogueira, T. Lindsten, A.M. Jamieson, C.L. Case, S. Shin, C.B. Thompson, et al., Rapid pathogen-induced apoptosis: a mechanism used by dendritic cells to limit intracellular replication of *Legionella pneumophila*, PLoS Pathog. 5 (2009) e1000478.
[19] J. Xu, S. Jiang, Y. Li, M. Li, Q. Cheng, D. Zhao, et al., Caspase-3 serves as an intracellular immune receptor specific for lipopolysaccharide in oyster *Crassostrea gigas*, Dev. Comp. Immunol. 61 (2016) 1–12.
[20] Y. Shao, C. Li, W. Zhang, X. Duan, Y. Li, C. Jin, et al., Molecular cloning and characterization of four caspases members in *Apostichopus japonicus*, Fish Shellfish Immunol. 55 (2016) 203–211.
[21] G. Zhang, X. Fang, X. Guo, L. Li, R. Luo, F. Xu, et al., The oyster genome reveals stress adaptation and complexity of shell formation, Nature 490 (2012) 49–54.
[22] T. Qu, L. Zhang, W. Wang, B. Huang, Y. Li, Q. Zhu, et al., Characterization of an inhibitor of apoptosis protein in *Crassostrea gigas* clarifies its role in apoptosis and immune defense, Dev. Comp. Immunol. 51 (2015) 74–78.
[23] C. Li, T. Qu, B. Huang, P. Ji, W. Huang, H. Que, et al., Cloning and characterization of a novel caspase-8-like gene in *Crassostrea gigas*, Fish Shellfish Immunol. 46 (2015) 486–492.
[24] G. Lu, Z. Yu, M. Lu, D. Liu, F. Wang, Y. Wu, et al., The self-activation and LPS binding activity of executioner caspase-1 in oyster *Crassostrea gigas*, Dev. Comp. Immunol. 77 (2017) 330–339.

[25] Y. Li, L. Zhang, T. Qu, X. Tang, L. Li, G. Zhang, Conservation and divergence of mitochondrial apoptosis pathway in the Pacific oyster, *Crassostrea gigas*, Cell Death. Dis. 8 (2017) e2915.
[26] K.J. Livak, T.D. Schmittgen, Analysis of relative gene expression data using real-time quantitative PCR and the 2(-Delta Delta C(T)) Method, Methods 25 (2001) 402–408.
[27] Z. Lv, L. Qiu, M. Wang, Z. Jia, W. Wang, L. Xin, et al., Comparative study of three C1q domain containing proteins from pacific oyster *Crassostrea gigas*, Dev. Comp. Immunol. 78 (2018) 42–51.
[28] A. Cao, L. Mercado, J.I. Ramos-Martinez, R. Barcia, Primary cultures of hemocytes from *Mytilus galloprovincialis* Lmk.: expression of IL-2Rα subunit, Aquaculture 216 (2003) 1–8.
[29] Z. Liu, L. Wang, Z. Lv, Z. Zhou, W. Wang, M. Li, et al., The cholinergic and adrenergic autocrine signaling pathway mediates immunomodulation in oyster *Crassostrea gigas*, Front. Immunol. 9 (2018) 284.
[30] Y.T. Zhu, D. Li, X. Zhang, X.J. Li, W.W. Li, Q. Wang, Role of transglutaminase in immune defense against bacterial pathogens via regulation of antimicrobial peptides, Dev. Comp. Immunol. 55 (2016) 39–50.
[31] H. Chen, H. Wang, S. Jiang, J. Xu, L. Wang, L. Qiu, et al., An oyster species-specific miRNA scaffold42648_5080 modulates haemocyte migration by targeting integrin pathway, Fish Shellfish Immunol. 57 (2016) 160–169.
[32] A. Oberst, C. Bender, D.R. Green, Living with death: the evolution of the mitochondrial pathway of apoptosis in animals, Cell Death Differ. 15 (2008) 1139–1146.
[33] A. Montesanti, K. Deignan, C. Hensey, Cloning and characterization of *Xenopus laevis* smac/DIABLO, Gene 392 (2007) 187–195.
[34] H. Steller, Regulation of apoptosis in *Drosophila*, Cell Death Differ. 15 (2008) 1132–1138.
[35] A. Kilar, A. Dornyei, B. Kocsis, Structural characterization of bacterial lipopolysaccharides with mass spectrometry and on- and off-line separation techniques, Mass Spectrom. Rev. 32 (2013) 90–117.
[36] M. Comalada, J. Xaus, A.F. Valledor, C. Lopez-Lopez, D.J. Pennington, A. Celada, PKC epsilon is involved in JNK activation that mediates LPS-induced TNF-alpha, which induces apoptosis in macrophages, Am. J. Physiol. Cell Physiol. 285 (2003) C1235–C1245.
[37] S. Yang, P. Li, Z. Mi, LPS-induced TNFα factor (LITAF) in the snail *Cipangopaludina chinensis*: gene cloning and its apoptotic effect on NCI-H446 cells, Fish Shellfish Immunol. 32 (2012) 268–272.
[38] C. Ren, T. Chen, H. Sun, X. Jiang, C. Hu, J. Qian, et al., The first echinoderm poly-U-binding factor 60 kDa (PUF60) from sea cucumber (*Stichopus monotuberculatus*): molecular characterization, inducible expression and involvement of apoptosis, Fish Shellfish Immunol. 47 (2015) 196–204.
[39] N. Yan, J.W. Wu, J. Chai, W. Li, Y. Shi, Molecular mechanisms of DrICE inhibition by DIAP1 and removal of inhibition by Reaper, Hid and Grim, Nat. Struct. Mol. Biol. 11 (2004) 420–428.
[40] A.G. Porter, R.U. Janicke, Emerging roles of caspase-3 in apoptosis, Cell Death Differ. 6 (1999) 99–104.
[41] C. Dou, N. Ding, J. Xing, C. Zhao, F. Kang, T. Hou, et al., Dihydroartemisinin attenuates lipopolysaccharide-induced osteoclastogenesis and bone loss via the mitochondria-dependent apoptosis pathway, Cell Death Dis. 7 (2016) e2162.